

Article

Low Temperature Sealing Process and Properties of Kovar Alloy to DM305 Electronic Glass

Zhenjiang Wang ¹, Zeng Gao ^{1,*}, Junlong Chu ¹, Dechao Qiu ¹ and Jitai Niu ^{1,2,3}

¹ School of Materials Science and Engineering, Henan Polytechnic University, Jiaozuo 454003, China; wangzhenjiang2017@163.com (Z.W.); chujunlong123@163.com (J.C.); qiu_dechao@163.com (D.Q.); niujitai@163.com (J.N.)

² State Key Laboratory of Advanced Welding and Joining, Harbin Institute of Technology, Harbin 150001, China

³ Henan Jingtai High-Novel Materials Ltd. of Science and Technology, Jiaozuo 454003, China

* Correspondence: mrgaozeng@163.com or gaozeng@hpu.edu.cn; Tel.: +86-138-3913-4383

Received: 12 June 2020; Accepted: 10 July 2020; Published: 13 July 2020



Abstract: The low temperature sealing of Kovar alloy to DM305 electronic glass was realized by using lead-free glass solder of the Bi₂O₃-ZnO-B₂O₃ system in atmospheric environment. The sealing process was optimized by pre-oxidation of Kovar alloy and low temperature founding of flake glass solder. The effects of sealing temperature and holding time on the properties of sealing joint were studied by means of X-ray diffraction (XRD), scanning electron microscope (SEM), energy dispersive X-ray spectroscopy (EDS), etc. The results showed that the pre-oxidized Kovar alloy and DM305 electronic glass were successfully sealed with flake glass solder at the sealing temperature of 500 °C for 20 min. Meanwhile, the joint interface had no pores, cracks, and other defects, the shear strength was 12.24 MPa, and the leakage rate of air tightness was 8×10^{-9} Pa·m³/s. During the sealing process, element Bi in glass solder diffused into the oxide layer of Kovar alloy and DM305 electronic glass about 1 μm, respectively.

Keywords: Kovar alloy; DM305 electronic glass; glass solder; low temperature sealing

1. Introduction

Glass materials have good light transmittance, insulation, and corrosion resistance, and many new applications and manufacturing processes will involve glass in combination with other materials [1]. Metal materials have good electrical conductivity, thermal conductivity, and plastic toughness. The comprehensive properties of glass and metal can be utilized through the combination of glass and metal. Glass to metal joints have been used in many applications. For example, glass insulation is required between the electronic package housing and the lead wire pin for microelectronic metal packaging [2–4]. A glass brazing material needs to be employed to seal between glass tube and metal pipe to achieve a certain degree of vacuum for parabolic trough receivers [5–8], and glass to metal sealing also plays a key role and can prevent the leakage of fuel and air in planar solid oxide fuel cells (SOFCs) [9–11]. Kovar alloy is a Fe-Ni-Co alloy with Fe as the main matrix element, and its expansion coefficient is similar to that of silicon-boron hard glass; therefore, Kovar alloy and glass sealing are widely used in the field of electronic packaging related to in-candescent lamps, electron tubes, and housing for semi-conductors [12]. However, Kovar alloy has high density, which is increasingly difficult to meet the light-weight requirements for modern electronic packaging [13]. Therefore, a new type of electronic packaging material is required. Aluminum metal matrix composites possess excellent performance such as light-weight, good thermal conductivity, and adjustable linear coefficient of thermal expansion, making them the first choice of the new generation electronic packaging materials [3,14,15].

As the current joining technology of new packaging materials is under development, it is extremely difficult to completely replace the traditional Kovar alloy with aluminum metal matrix composites in a short period of time. However, the use of a combination of aluminum metal matrix composites and Kovar alloy can be designed to achieve weight reduction of the packaging shell, as shown in Figure 1. For example, the phased array radar T/R module was generally made of Kovar alloy. If a high-volume fraction silicon carbide reinforced aluminum matrix composite (65% SiC_p/Al-MMCs) with a similar low expansion coefficient is employed, the phased array radar can get a weight loss of about 2/3 [16]. For the T/R module sealing component of electronic packaging shell and glass insulation terminal, a part of 65% SiC_p/Al-MMCs is utilized to replace Kovar alloy, which can achieve a significant weight reduction of the packaging shell and at the same time is of great performance promotion. In addition, it is also a great economic value. In the past, the sealing of Kovar alloy with glass-insulated terminals (DM305 electronic glass) was generally carried out in three steps, that were, decarburization and degassing in humid hydrogen environment with high temperature, surface pre-oxidation treatment and sintering with glass. The sealing process of Kovar alloy to glass at high temperatures has been extensively studied by scholars. Luo et al. [17] studied the wetting and spreading behavior of borosilicate glass on the surface of pre-oxidized Kovar alloy, and proposed three wetting stages: incubation period, reaction period and equilibrium period. Kuo et al. [12] realized the matching sealing of ASF series glass to pre-oxidized Kovar alloy under the protection of inert gas, and the sealing strength of ASF110 glass to Kovar alloy was about 3.9 MPa. The pre-oxidation of Kovar was a key factor for sealing. During the pre-oxidation of Kovar alloy, FeO, Fe₃O₄, Fe₂O₃ and (Fe, Co, Ni)₃O₄ would appear in the oxide layer [18,19], but the main oxide was FeO. After pre-oxidization, metallic oxide layer will be generated on the surface of Kovar alloy. As it is well known, the chemical bond type of metallic oxide is ionic bond. Meanwhile, the chemical bond of DM305 electronic glass is a mixture of ionic and covalent bond. As a consequence, the low temperature glass which had a similar chemical bond could be employed in theory as an intermediate solder to join Kovar alloy and DM305 electronic glass, which was expected to realize a new packaging process of metal and glass.

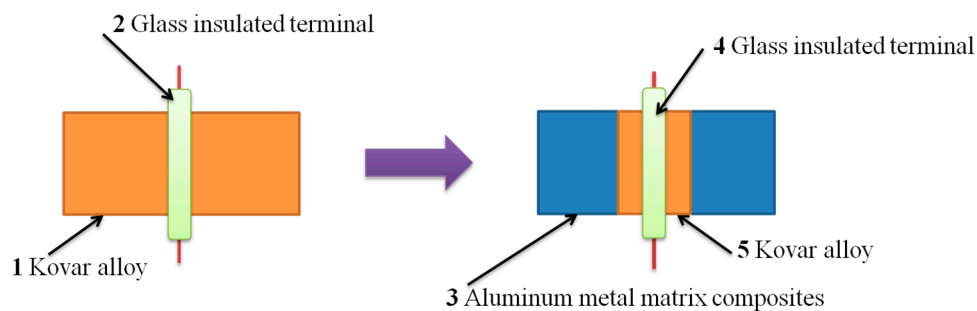


Figure 1. Schematic diagram of composite component formed by aluminum metal matrix composites replacing part of Kovar alloy.

The traditional sealing process is complicated and requires multiple high-temperature processes, wasting energy. In addition, high temperatures inevitably cause damage to the base metal of Kovar and glass-insulated terminals. More importantly, when the composite component involving aluminum metal matrix composites and Kovar alloy are sealed with glass-insulated terminal, it is no longer feasible to use traditional sintering at high temperature of 1000 °C since the melting point of aluminum is only 660 °C. New sealing methods are urgently needed. Due to environmental protection requirements, lead-free green glass powder will be used in large quantities replacing traditional lead-containing glass powder which is banned by many countries [20–24]. Simultaneously, some scholars have successfully combined sapphire, aluminum ceramics, Li–Ti ferrite, and other materials using lead-free glass solder in recent years [25–29]. In this study, low-temperature green glass powder Bi₂O₃-ZnO-B₂O₃ system which has similar chemical bonding with the pre-oxidized Kovar alloy surface and DM305 electronic glass was employed as a solder to achieve the sealing of Kovar alloy to DM305 electronic glass at

low temperature, aiming to solve the problem of sealing aluminum metal matrix composites and Kovar alloy composite component with glass-insulated terminals, and to promote the application of aluminum composite materials in the field of electronic packaging. To use low-temperature green glass powder not only has a simple process and energy saving, but also responds to the world's call for green materials according to Waste Electrical and Electronic Equipment (WEEE) Directive and the Restriction of Hazardous Substances (RoHS) Directive in Electrical and Electronic Equipment [30].

2. Materials and Methods

2.1. Materials Preparation and Sealing Process

The specimens with the size of $15 \times 10 \times 2$ mm were machined from the 4J29 Kovar alloy, whose composition was Ni 29.0 wt.%, Co 17.2 wt.%, Mn 0.3 wt.%, Si 0.2 wt.%, C 0.02 wt.%, with Fe balanced. Each surface of the flake samples was polished by 800 grade metallographic papers, and then ultrasonically cleaned in acetone for 10 min and in alcohol for 15 min, respectively. After being dried, the Kovar alloy samples were placed into a resistance furnace (GWL-1200), which was also employed for sealing test, and the temperature control accuracy was ± 1 °C. The samples were firstly heated up to 900 °C at the rate of 15 °C/min and to be held for 1 min for pre-oxidation in air. The commercially available DM305 electronic glass had the same size as Kovar alloy. Its nominal composition was Al₂O₃ 3.5 wt.%, B₂O₃ 20.3 wt.%, K₂O 4.9 wt.%, Na₂O 3.8 wt.%, Fe₂O 30.1 wt.%, with SiO₂ balanced. The composition of Bi₂O₃-ZnO-B₂O₃ system glass solder utilized in the research is shown in Table 1. The coefficient of thermal expansion (CTE) of three categories of materials used in this work are shown in Table 2.

Table 1. Chemical compositions of glass solder (in wt.%).

Composition	Bi ₂ O ₃	ZnO	B ₂ O ₃	Na ₂ CO ₃	SiO ₂
Content	70–80	0–10	0–10	0–5	0–5

Table 2. Coefficient of thermal expansion of 4J29 Kovar alloy, DM305 electronic glass and glass solder.

Material	4J29 Kovar Alloy	DM305 Electronic Glass	Glass Solder
CET $\times 10^{-7}/^{\circ}\text{C}$	5.1–5.5	4.8–5.0	6.5–7.5

In order to avoid air pore defects caused by air gaps in the powder solder during the sealing process, the powder solder was putted in a self-designed mold first, as shown in Figure 2a. Then the mold was heated from room temperature to 200 °C at the rate of 10 °C/min and held for 10 min. Subsequently, it was heated to 460 °C at the rate of 10 °C/min and held for 30 min in the resistance furnace surrounded by atmosphere environment. After that, the glass column ($\varphi 5 \times 3$ mm) prepared for wetting experiment and flake glass solder ($7.5 \times 7.5 \times 0.5$ mm) used for sealing were obtained. The wetting experiment was carried out by classical sessile drop method. The glass column was placed in the middle of pre-oxidized Kovar and DM305 electronic glass primarily, then the specimens were heated directly up to 480, 500, 520, 540 and 560 °C at the rate of 10 °C/min and held for 30 min in the resistance furnace, respectively. The sandwich specimen assembled in a sealing fixture is shown in Figure 2b, the overlap length was 10 mm. During sealing process, the pressure of 0.01 MPa was applied to the sandwich specimen. The self-designed device in Figure 2c was used for joint shear test. The sealing experiments were performed by heating the specimens in the resistance furnace in air. Figure 3 shows the process of sealing. The sandwich specimen was firstly heated up to 250 °C at the rate of 10 °C/min and held for 10 min to keep temperature uniform and reduce thermal stress. Then the specimen was continually heated up to sealing temperature at the rate of 5 °C/min and held for 10~40 min. After that, the specimen was cooled down to 350 °C at the rate of 5 °C/min, and then

was cooled down to room temperature in furnace. Sealing processes of Kovar alloy to DM305 electronic glass are listed in Table 3.

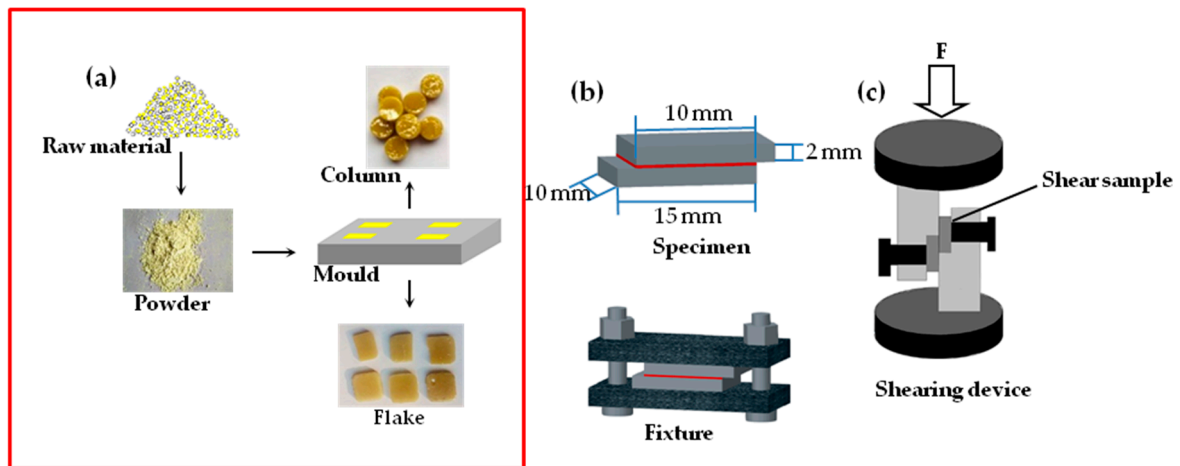


Figure 2. Schematic diagrams of experimental procedure: (a) Glass powder molding process, (b) sealing assembly, and (c) shear testing.

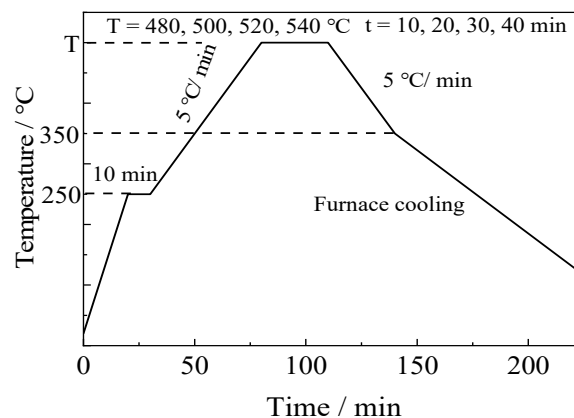


Figure 3. Process of sealing with different sealing temperatures and holding times.

Table 3. Sealing processes of Kovar alloy to DM305 electronic glass.

Sealing Temperature/°C	Holding Time/min	Sealing Pressure/MPa	Glass Solder
480	20	0.01	flake
500	20	0.01	flake
520	20	0.01	flake
540	20	0.01	flake
500	10	0.01	flake
500	30	0.01	flake
500	40	0.01	flake

2.2. Characterization Methods

Before the sealing experiments, thermophysical properties of the glass solder were analyzed by differential scanning calorimetry (DSC, Q100, TA Instruments, New Castle, DE, USA). Shearing test of the sealing joint was performed at a constant rate of 0.02 mm/min by using an electronic universal testing machine (CMT5105, MTS Systems (China) Co., Ltd., Shenzhen, China) at room temperature. Three samples were employed for each experiment condition, and the adopted shear strength was the average of the three samples. The wettability of the glass solder on base material was observed by metallographic microscope (OLYMPUS GX51, Olympus Corporation, Tokyo, Japan). The microstructure and elements

composition of the joints were carried out by scanning electron microscope (SEM, Carl Zeiss NTS GmbH, Merlin Compact, Jena, Germany) coupled with energy dispersive X-ray spectroscopy (EDS). The phases in joint were analyzed by X-ray diffraction (XRD, Dmax-RB, Rigaku Corporation, Tokyo, Japan). To evaluate the effectiveness of sealing process, air tightness of the joint was measured with a ZQJ-530 helium leak mass spectrometer (KYKY Technology Development Ltd., Beijing, China). The final air tightness value was selected from the worst one among three tested samples for each experiment condition.

3. Results and Discussion

3.1. Thermophysical Properties of $\text{Bi}_2\text{O}_3\text{-ZnO-B}_2\text{O}_3$ System Glass

The DSC curve of the glass solder is shown in Figure 4. The temperature and meaning of each feature point on the curve are shown in Table 4. According to the analysis of DSC curve, the glass transition temperature (T_g) of the glass solder is 350 °C and the softening temperature (T_f) is 429 °C, respectively. Based on Ma Yingren's research on low-melting glass, to fully wet the sealing interface of the base material, the viscosity of low-temperature glass must reach $10^3\text{--}10^5$ Pa·s. To reach this viscosity, the sealing temperature was generally set to be higher than the softening point in a range of 50–100 °C [31]. As a consequence, the sealing temperature in this research was set to be in the range of 480–560 °C based on DSC analysis of $\text{Bi}_2\text{O}_3\text{-ZnO-B}_2\text{O}_3$ system.

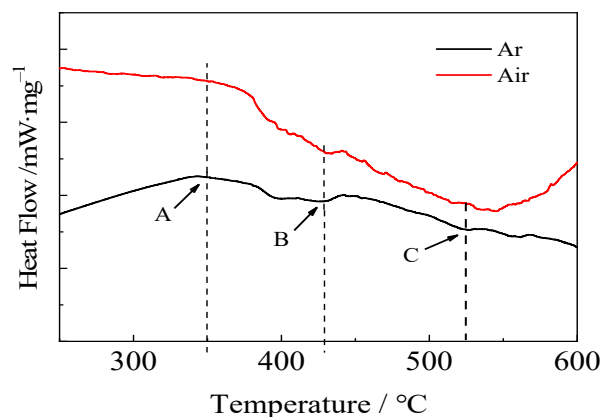


Figure 4. Differential scanning calorimetry (DSC) curve of the $\text{Bi}_2\text{O}_3\text{-ZnO-B}_2\text{O}_3$ system glass solder.

Table 4. Temperatures and meanings of the points on DSC curve in Figure 4.

Point	Temperature/°C	Meaning
A	350	Glass transition point
B	429	Glass softening point
C	520	Glass flow point

Within the heating process, the first obvious exothermic peak appeared when the temperature had reached about 440 °C, which indicated that crystallization may occur in the heating process. In order to further verify the above analysis, powdered and flaky glass solders were prepared for XRD analysis. Figure 5 shows that the powdered glass solder was amorphous, but a small amount of crystallization occurred in the flaky glass solder which was founded at 460 °C for 30 min, and the crystalline phase was mainly Bi_2O_3 . As presented in Table 1, the content of Bi_2O_3 in glass solder was high. As a result, the amorphous phase of Bi_2O_3 in a thermodynamic metastable state partially crystallized more likely during the heating process.

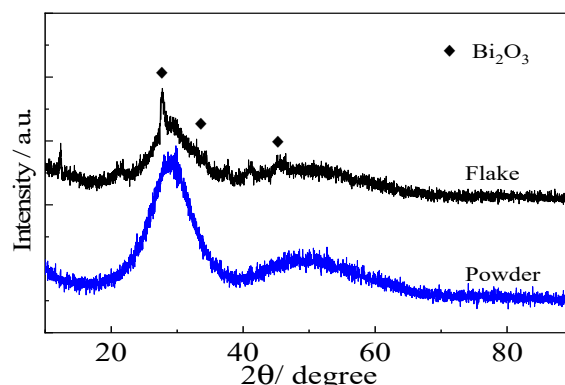


Figure 5. XRD patterns of the powder and flake glass solder.

The wetting angle reflects the bonding ability of the glass solder to base material. A reasonable sealing temperature range could be chosen according to the wetting angle of glass solder on two base materials at different temperatures. Figure 6 is a typical wetting physical and metallographic picture of the glass solder on both base materials at a temperature of 500 °C for 20 min. It can be seen that the glass solder had formed a good interface bonding with Kovar and DM305 electronic glass, respectively. The wetting angle on Kovar alloy was 38° which was smaller than that on DM305 electronic glass 65°, and both were less than 90°, indicating that this glass solder could wet the two of base materials and the sealing process was possible.

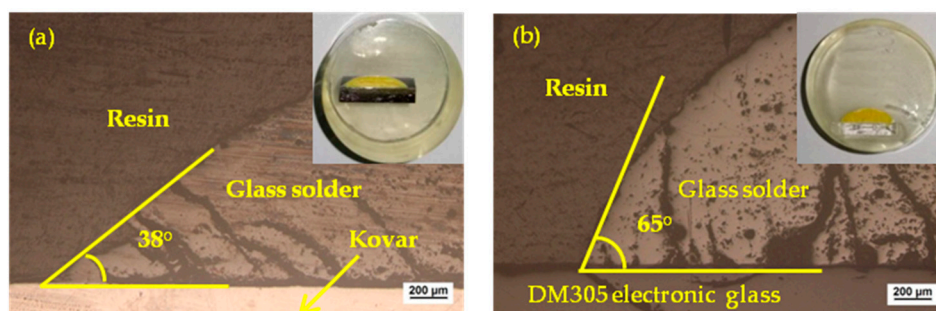


Figure 6. Typical wetting images of glass solder on base materials at 500 °C for 20 min: (a) Glass solder/Kovar and (b) glass solder/DM305 electronic glass.

Figure 7 shows the wetting angles of the glass solder on base materials at different temperatures for 20 min. It could be seen that the wetting angle of the glass solder on each material was larger than 90° at 480 °C, suggesting the glass solder had a poor wettability on each base material. When the temperature increased to 500 and 520 °C, the wetting angle decreased significantly as the viscosity of glass solder decreased rapidly as the temperature rose. During the temperature range of 540 to 560 °C, the wetting angle on electronic glass did not change significantly, but there was an obvious "collapse" for Kovar alloy at 560 °C whether it was pre-oxidized or not, and the wetting angle was reduced to 20°, reaching a minimum. Whether the Kovar alloy underwent pre-oxidation treatment had little effect on wetting angle when the temperature exceeded 540 °C. It could be explained that when the temperature continued to increase after 540 °C, the viscosity of glass solder decreased accordingly, and the change of viscosity was the main factor that promoted wetting, while the surface state of Kovar alloy had little effect on wetting. It was generally considered that the wetting angle was suitable for sealing in the range of 45° to 90° [32]. Therefore, it was speculated that the reasonable sealing temperature range was from 500 to 540 °C in this research.

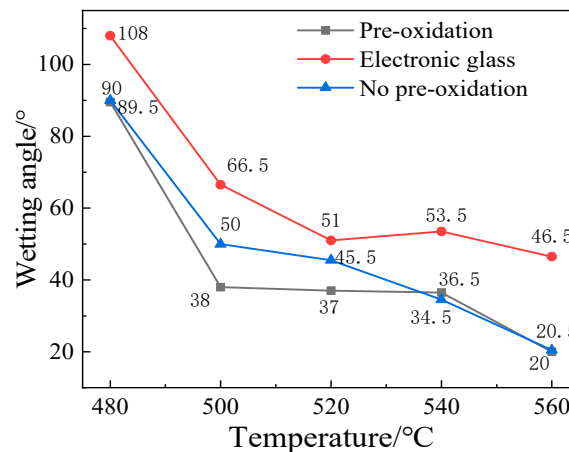


Figure 7. Wetting angle between glass solder and different base metals at different temperatures for 20 min.

3.2. Effect of Sealing Temperature on Sealing Joint Microstructure Evolution

In order to investigate the effect of sealing temperature on microstructure evolution of the sealing joints, the joints were sealed using the temperatures of 480, 500, 520 and 540 °C with a constant holding time of 20 min. The SEM micrographs of the joints are shown in Figure 8. Figure 8a shows the secondary electronic image of the sealing joint obtained under the condition of sealing temperature 480 °C. It could be seen that the bonding between DM305 electronic glass and Kovar alloy was achieved. There were a small number of pores in the joint. The primary reason was that the low sealing temperature could result in the difficulty of venting gas due to the poor fluidity of glass solder. When the sealing temperature was 500 °C, as can be seen in Figure 8b. The joint could be divided into three regions: zone 1 at the bonding area between DM305 electronic glass and glass solder, zone 2 in the middle of the sealing joint and zone 3 at the bonding area between Kovar alloy and glass solder. Additionally, there were three kinds of interface between base metal and glass solder: Kovar–oxide layer, oxide layer–glass solder and DM305 electronic glass–glass solder, and each interface was well bonded. In zone 1, the interface between DM305 electronic glass–glass solder was smooth, which was due to original small surface roughness of DM305 electronic glass which could not be melt during the sealing process for its high softening point. There were no obvious cracks and pores at the interface, and some fine gray-white crystals generated. Zone 2 was an obvious $\text{Bi}_2\text{O}_3\text{-ZnO-B}_2\text{O}_3$ glass solder, with a few small pores and a small amount of gray-white crystal phases. In zone 3, a black oxide film which bonded the glass solder to Kovar alloy together formed after pre-oxidation, and the interface of glass solder–oxide film combined well. There were fine gray crystals at the interface, without obvious cracks, pores, and other defects. The interface between oxide film–Kovar alloy was also compact, and there was a small amount of fine oxide embedded into the fringe area of Kovar alloy.

Figure 8c shows the sealing joint obtained at the sealing temperature of 520 °C. It could be found that there were obvious cracks on the Kovar–oxide layer interface, and the sizes of the pores in the center of the sealing joint were obviously increased. Meanwhile, the sizes of crystal phases were larger with an average diameter about 20 μm compared to the previous with an average diameter about 10 μm in Figure 8b. The number of crystal phases at interface on both sides decreased, while the number of crystalline phases in the center of the joint increased, which may be due to the partial melting of the crystalline phase at the interface. When the sealing temperature was 540 °C, as shown in Figure 8d, there were large pores that penetrated the entire joint due to high temperature which caused the glass solder to be over-burned. Accordingly, the pores decreased the performance of the sealing joint significantly.

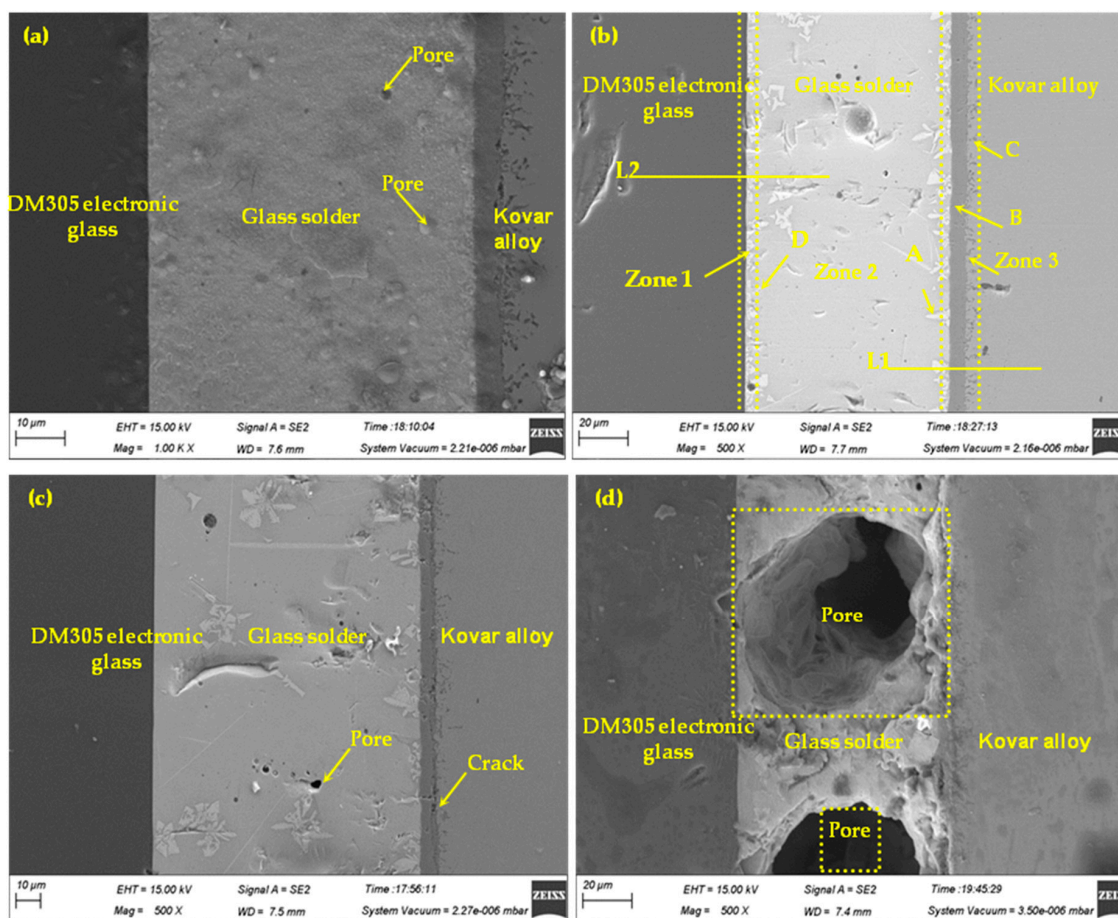


Figure 8. SEM images of the typical sealing joints at different sealing temperatures for 20 min: (a) 480 °C, (b) 500 °C, (c) 520 °C, and (d) 540 °C.

The point energy spectrum positions are shown in Figure 8b and the results and possible phases or matters in the joint are listed in Table 5. XRD analysis was performed to further confirm the phases in the joint. As can be seen, compared with the original glass powder shown in Figure 5, Bragg diffraction peaks could be also observed from the XRD pattern besides the amorphous peak, as shown in Figure 9. Therefore, the gray-white crystal phase A was $\text{Bi}_{24}\text{B}_2\text{O}_{39}$ according to the results of XRD analysis and the point energy spectrum, and this is consistent with the result in the previous literature [33]. It could be speculated that point B was mainly a FeO oxide layer of Kovar alloy, point C contained point FeO oxide and a matrix of Kovar alloy, and point D was glass solder, respectively, in Table 5.

Table 5. Energy dispersive X-ray spectroscopy (EDS) analysis of points at the interface of the sealing joint in Figure 8b (in wt.%).

Point	Fe	Co	Ni	O	Bi	B	Zn	Possible Phases or Matters
A	-	-	-	9.0	85.9	5.1	-	$\text{Bi}_{24}\text{B}_2\text{O}_{39}$
B	59.6	7.8	-	32.6	-	-	-	FeO
C	58.6	6.0	7.4	28.0	-	-	-	FeO, Kovar
D	-	-	-	10.1	82.8	4.1	3.0	Glass solder

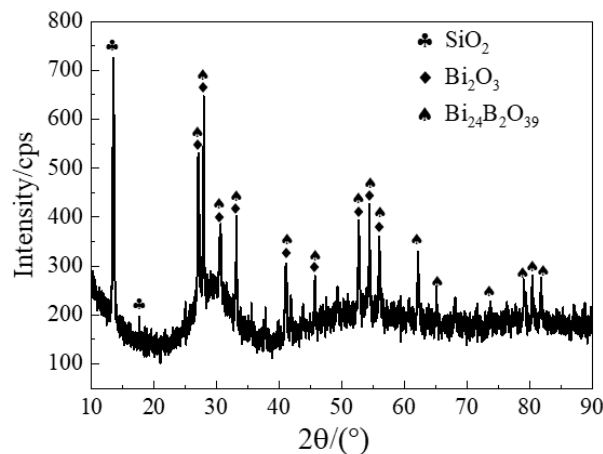


Figure 9. XRD patterns of the sealing joint in Figure 8b.

Simultaneously, line scanning analysis of the main elements was performed at marked positions in Figure 8b. At the L1 line scanning position, as shown in Figure 10a, the diffusion and dissolution layer were found to be relatively thin, about 1 μm . The thickness of oxide layer on Kovar alloy was about 6 μm . Due to the slight dissolution of oxide layer into glass solder, the element of Fe was distributed in the gradient of its diffusion and dissolution layer. At the same time, the element of Bi also diffused slightly from the glass solder layer into the oxide layer, about 1 μm . Similarly, at the DM305 electronic glass–glass solder interface, line scan analysis for the main elements was also performed at the marked position of line L2, as shown in Figure 10b. At the sealing temperature of 500 $^{\circ}\text{C}$, only the glass solder melted, so the diffusion and dissolution layer were relatively thin. At the interface of DM305 electronic glass–the glass solder, there was a certain gradient distribution of Si, Bi, and O elements, and the diffusion distance of Si and O elements was about 2 μm , while that of Bi element was about 1 μm . It was noteworthy that there was a certain Bi element enrichment at the front of the interface of the glass solder–oxide layer and the same at the front of the interface of the glass solder–DM305 electronic glass, which was mainly due to the existence of Bi-rich crystalline phases at the front of the interface.

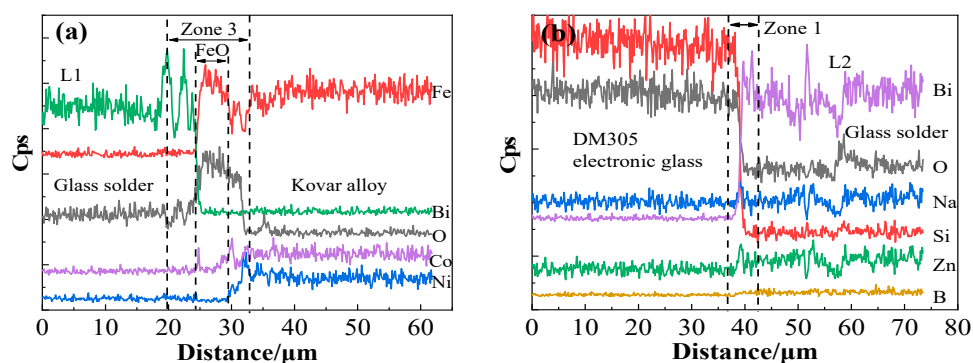


Figure 10. EDS line scanning of glass solder–Kovar alloy (a) and DM305 electronic glass–glass solder (b) of the sealing joint in Figure 8b.

3.3. Shear Tests of Sealing Joints

In order to find the best sealing process, the effects of sealing temperature and holding time on mechanical properties of sealing joints were studied, respectively, as shown in Figure 11a (fixed holding time 20 min) and Figure 11b (fixed sealing temperature 500 $^{\circ}\text{C}$). As the sealing temperature increased, the joint shear strength increased firstly and then decreased, and reached a peak value of 12.24 MPa at 500 $^{\circ}\text{C}$. This was mainly because the glass solder was not dense enough and not fully spread out at low temperature, since the viscosity of solder was too high and element diffusion ability at interface was weak. Meanwhile, there were a certain number of pores that were not expelled out in time in the joint,

resulting in low interface bonding strength as well, as can be seen in Figure 8a. On the contrary, when the temperature was too high, the occurrence of glass solder over-burning caused enormous porosity, which reduced the shear strength too, as can be seen in Figure 8d.

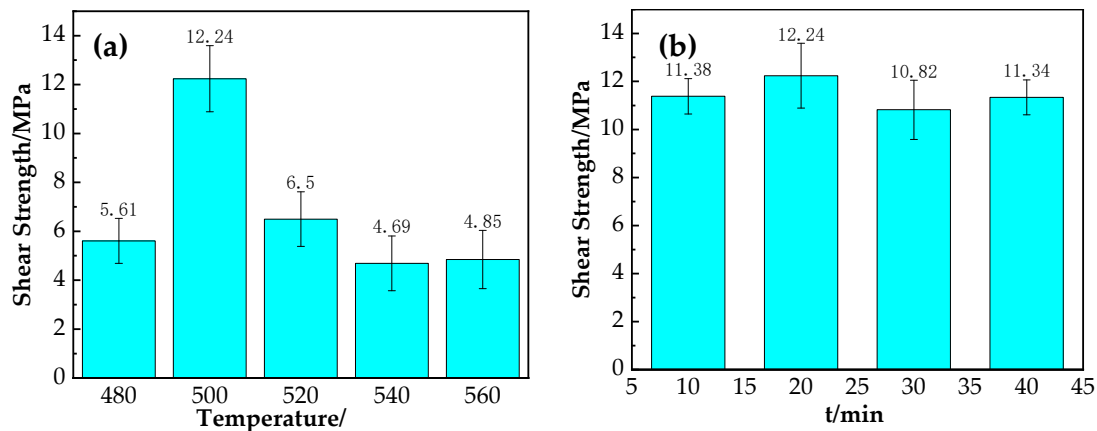


Figure 11. Effect of temperature (a) and holding time (b) on shear strength of the sealing joints.

Similarly, the changing trend of shear strength with the holding time changed was also studied, as shown in Figure 11b. In general, the shear strength did not change much with time; when the holding time was 20 min, the joint strength reached a peak value of 12.24 MPa. It could be speculated that the element diffusion was not sufficient when holding time was short. Instead, if the holding time was too long, the number and size of the crystalline phases would become more and larger, reducing the performance of the joint correspondingly. In order to further understand the mechanism of shear fracture, A typical force–displacement curve was displayed, as shown in Figure 12. The maximum shear load was 1256.29 N, and the shear strength was 12.56 MPa. The force–displacement curve was almost straight and no yield. Therefore, the sample belonged to brittle fracture with no obvious shear deformation.

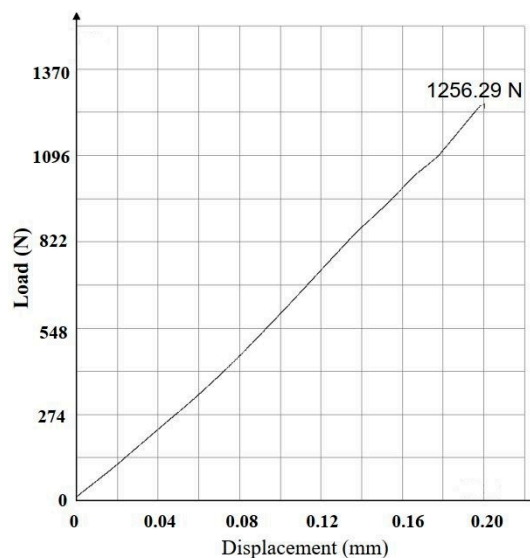


Figure 12. Typical force–displacement curve of the joint made at 500 °C for 20 min.

3.4. Air Tightness Tests of Sealing Joints

Air tightness is one of the most important factors affecting electronic packaging devices. By testing air tightness of the joint, the bonding condition of sealing interface can be evaluated from the air tightness, and it can also reflect the compactness of the oxide layer of Kovar alloy to a certain extent.

The air tightness of the sample is up to standard if the air leakage rate is less than 1×10^{-7} Pa·m³/s according to Chinese national standard (GB 5594. 1-85, Air Tightness Test Method). Table 6 lists the air tightness of the sealing joint under different sealing temperatures for 20 min.

Table 6. Air tightness of samples at different temperatures for 20 min.

Temperatures/°C	480	500	520	540	560
Leakage rate/Pa·m ³ /s	9×10^{-8}	8×10^{-9}	7×10^{-8}	6×10^{-7}	4×10^{-7}

The air tightness of the samples was up to standard when the sealing temperature was from 480 to 520 °C, but it was not qualified when the sealing temperature was higher than 520 °C, because the bonding temperature was too high and a large number of pores appeared in the solder. Meanwhile, the effect of holding time on the air tightness of the samples was also studied. It was found that the air tightness of all samples could meet the application requirements when the sealing temperature was 500 °C for 10~40 min, as shown in Table 7, indicating that the holding time had little effect on the air tightness of the samples.

Table 7. Air tightness of samples with different times at 500 °C.

Times/min	10	20	30	40
Leakage rate/Pa·m ³ /s	5×10^{-8}	8×10^{-9}	6×10^{-8}	8×10^{-8}

4. Conclusions

In this work, Kovar alloy and DM305 electronic glass were successfully sealed by lead-free low temperature flake glass solder in atmospheric environment. Thermophysical properties, microstructure, shear testing, and air tightness testing of the joints were analyzed to confirm the performance of the sealing joints. This new low temperature sealing process can provide some technical reference and theoretical value for solving the problem of sealing aluminum metal matrix composites and Kovar alloy composite component to glass-insulated terminals, promoting the application of aluminum composite materials in the field of electronic packaging to some extent. The main results are as follows:

(1) The glass transition temperature T_g was 350 °C and softening temperature T_f was 429 °C for the Bi₂O₃-ZnO-B₂O₃ system lead-free glass solder. When the holding time was unchanged for 20 min, the wetting angle of the glass solder on both base materials was less than 90° after the temperature reached 500 °C, whereas the wetting angle was larger than 90° at 480 °C. Therefore, the glass solder had a good wettability on both base materials when the temperature was higher than 500 °C.

(2) The Bi₂O₃-ZnO-B₂O₃ system lead-free glass solder can realize the low temperature sealing of Kovar alloy to DM305 electronic glass. When the sealing temperature increased from 480 to 560 °C, the joint shear strength increased firstly and then decreased gradually. The maximum joint shear strength of 12.24 MPa can be reached when the sealing temperature of 500 °C and holding time of 20 min were utilized. Simultaneously, the joint air tightness could meet the application requirements.

(3) During the sealing process, crystallization of the Bi₂O₃-ZnO-B₂O₃ system glass solder appeared, and the crystal phases included Bi₂₄B₂O₃₉, Bi₂O₃, and SiO₂. At the sealing temperature of 500 °C, the crystallization mainly occurred at the interface between the glass solder and the base material. When the temperature reached to 520 °C, the crystallization phases at the interface decreased and gradually were transferred to the center of the joint.

(4) The mechanism of sealing mainly depends on short-range diffusion of some elements, such as Fe, Si, Bi and O elements, at the interface that lead to formation of an effective bonding between the glass solder and the base material according to line scan analysis.

Author Contributions: Investigation, Z.W., Z.G. and J.C.; resources, J.C. and D.Q.; supervision, J.N.; writing—original draft preparation, Z.W.; writing—review and editing, Z.G. and J.N. All authors have read and agreed to the published version of the manuscript.

Funding: The research was financially supported by the National Natural Science Foundation of China (No.51245008), the Science and Technology Project of Henan Province, China (No. 202102210036), the Fundamental Research Funds for the Universities of Henan Province, China (No. NSFRF180405).

Conflicts of Interest: The authors declare no conflict of interest.

References

1. Axinte, E. Glasses as engineering materials: A review. *Mater. Des.* **2011**, *32*, 1717–1732. [[CrossRef](#)]
2. Chanmuang, C.; Naksata, M.; Chairuangri, T.; Jain, H.; Lyman, C. Microscopy and strength of borosilicate glass-to-Kovar alloy joints. *Mater. Sci. Eng. A* **2008**, *474*, 218–224. [[CrossRef](#)]
3. Wang, P.; Xu, D.; Niu, J. Vacuum brazing of electroless Ni–P alloy-coated SiCp/Al composites using aluminum-based filler metal foil. *Appl. Phys. A* **2016**, *122*, 122. [[CrossRef](#)]
4. Staff, M.; Fernie, J.A.; Mallinson, P.M.; Whiting, M.; Yeomans, J. Fabrication of a Glass-Ceramic-to-Metal Seal Between Ti-6Al-4V and a Strontium Boroaluminate Glass. *Int. J. Appl. Ceram. Technol.* **2016**, *13*, 956–965. [[CrossRef](#)]
5. Joshi, R.; Chhibber, R. Development and interface characterization of unmatched glass-metal joint. *J. Manuf. Process.* **2018**, *31*, 787–800. [[CrossRef](#)]
6. Joshi, R.; Chhibber, R. Failure Study of Compression Glass-Metal Joint for Parabolic Trough Receiver Tube application. *Mater. Today Proc.* **2018**, *5*, 14847–14851. [[CrossRef](#)]
7. Joshi, R.; Chhibber, R. High temperature wettability studies for development of unmatched glass-metal joints in solar receiver tube. *Renew. Energy* **2018**, *119*, 282–289. [[CrossRef](#)]
8. Lei, D.; Wang, Z.; Li, J.; Li, J.; Wang, Z. Experimental study of glass to metal seals for parabolic trough receivers. *Renew. Energy* **2012**, *48*, 85–91. [[CrossRef](#)]
9. Yan, J.; Wu, Y.; Lin, D.; Zhan, H.; Zhuang, H.; Sa, B.; Zhang, T. Structural transformation-induced surface strengthening of borosilicate sealing glass for solid oxide fuel cells. *Ceram. Int.* **2019**, *45*, 15629–15635. [[CrossRef](#)]
10. Smeacetto, F.; De Miranda, A.; Ventrella, A.; Salvo, M.; Ferraris, M. Shear strength tests of glass ceramic sealant for solid oxide fuel cells applications. *Adv. Appl. Ceram.* **2015**, *114*, 70. [[CrossRef](#)]
11. Javed, H.; Sabato, A.G.; Dlouhy, I.; Halasova, M.; Bernardo, E.; Salvo, M.; Herbrig, K.; Walter, C.; Smeacetto, F. Shear Performance at Room and High Temperatures of Glass–Ceramic Sealants for Solid Oxide Electrolysis Cell Technology. *Materials* **2019**, *12*, 298. [[CrossRef](#)] [[PubMed](#)]
12. Kuo, C.-H.; Cheng, P.-Y.; Chou, C.-P. Matched glass-to-Kovar seals in N₂ and Ar atmospheres. *Int. J. Miner. Met. Mater.* **2013**, *20*, 874–882. [[CrossRef](#)]
13. Zhang, S.; Xu, X.; Lin, T.; He, P. Recent advances in nano-materials for packaging of electronic devices. *J. Mater. Sci. Mater. Electron.* **2019**, *30*, 13855–13868. [[CrossRef](#)]
14. Wang, P.; Xu, D.; Zhai, Y.; Niu, J. The dissimilar brazing of Kovar alloy to SiCp/Al composites using silver-based filler metal foil. *Appl. Phys. A* **2017**, *123*, 569. [[CrossRef](#)]
15. Garg, P.; Jamwal, A.; Kumar, D.; Sadasivuni, K.K.; Hussain, C.M.; Gupta, P. Advance research progresses in aluminium matrix composites: Manufacturing & applications. *J. Mater. Res. Technol.* **2019**, *8*, 4924–4939. [[CrossRef](#)]
16. Wang, P.; Gao, Z.; Li, J.; Cheng, D.; Niu, J. Research on reaction brazing of Ti layer-coated SiCp/Al composites using Al-based filler metal foil. *Compos. Interfaces* **2019**, *26*, 1057–1068. [[CrossRef](#)]
17. Luo, D.; Shen, Z. Wetting and spreading behavior of borosilicate glass on Kovar. *J. Alloy. Compd.* **2009**, *477*, 407–413. [[CrossRef](#)]
18. Chern, T.-S.; Tsai, H.-L. Wetting and sealing of interface between 7056 Glass and Kovar alloy. *Mater. Chem. Phys.* **2007**, *104*, 472–478. [[CrossRef](#)]
19. Yates, P.M.; Mallinson, C.; Mallinson, P.M.; Whiting, M.; Yeomans, J. An Investigation into the Nature of the Oxide Layer Formed on Kovar (Fe–29Ni–17Co) Wires Following Oxidation in Air at 700 and 800 °C. *Oxid. Met.* **2017**, *88*, 733–747. [[CrossRef](#)]
20. Wang, F.; Dai, J.; Shi, L.; Huang, X.; Zhang, C.; Li, X.; Wang, L. Investigation of the melting characteristic, forming regularity and thermal behavior in lead-free V2O5–B2O3–TeO2 low temperature sealing glass. *Mater. Lett.* **2012**, *67*, 196–198. [[CrossRef](#)]

21. Fredericci, C.; Yoshimura, H.; Molisani, A.; Fellegara, H. Effect of TiO₂ addition on the chemical durability of Bi₂O₃–SiO₂–ZnO–B₂O₃ glass system. *J. Non-Crystalline Solids* **2008**, *354*, 4777–4785. [[CrossRef](#)]
22. He, F.; Wang, J.; Deng, D. Effect of Bi₂O₃ on structure and wetting studies of Bi₂O₃–ZnO–B₂O₃ glasses. *J. Alloy. Compd.* **2011**, *509*, 6332–6336. [[CrossRef](#)]
23. Hong, J.; Zhao, D.; Gao, J.; He, M.; Li, H.; He, G. Lead-free low-melting point sealing glass in SnO–CaO–P₂O₅ system. *J. Non-Crystalline Solids* **2010**, *356*, 1400–1403. [[CrossRef](#)]
24. Yang, Y.; Wu, L.; Teng, Y.; Jiang, F.; Lei, J.; Chen, H.; Cheng, J. Effect of ZnO content on microstructure, crystallization behavior, and thermal properties of xZnO–30B₂O₃–(65–x)Bi₂O₃–5BaO glass. *J. Non-Crystalline Solids* **2019**, *511*, 29–35. [[CrossRef](#)]
25. Guo, W.; Fu, L.; He, P.; Lin, T.; Wang, C. Crystallization and wetting behavior of bismuth–borate–zinc glass and its application in low temperature joining alumina ceramics. *J. Manuf. Process.* **2019**, *39*, 128–137. [[CrossRef](#)]
26. Guo, W.; Wang, T.; Lin, T.; Guo, S.; He, P. Bismuth borate zinc glass braze for bonding sapphire in air. *Mater. Charact.* **2018**, *137*, 67–76. [[CrossRef](#)]
27. Lin, P.; Lin, T.; He, P.; Guo, W.; Wang, J. Investigation of microstructure and mechanical property of Li–Ti ferrite/Bi₂O₃–B₂O₃–SiO₂ glass/Li–Ti ferrite joints reinforced by FeBi₅Ti₃O₁₅ whiskers. *J. Eur. Ceram. Soc.* **2015**, *35*, 2453–2459. [[CrossRef](#)]
28. Lin, P.; Lin, T.; He, P.; Sekulic, D.P. Wetting behavior and bonding characteristics of bismuth-based glass brazes used to join Li–Ti ferrite systems. *Ceram. Int.* **2017**, *43*, 13530–13540. [[CrossRef](#)]
29. Lin, P.; Wang, C.; He, P.; Wang, T.; Guo, W.; Lin, T. Brazing of Al₂O₃ ceramics by Bi₂O₃–B₂O₃–ZnO glass. *Procedia Manuf.* **2019**, *37*, 261–266. [[CrossRef](#)]
30. Zhang, L.; Han, J.-G.; He, C.-W.; Guo, Y.-H. Reliability behavior of lead-free solder joints in electronic components. *J. Mater. Sci. Mater. Electron.* **2012**, *24*, 172–190. [[CrossRef](#)]
31. Ma, Y. Sealing glass seven-low melting glass. *Glass Enamel.* **1993**, *21*, 50–54. (In Chinese)
32. Wang, J.; He, F.; Deng, D.; Tan, M. Research on Bismuth Glass and Stainless Steel Wettability. *J. Wuhan Univ. Technol.* **2010**, *32*, 60–64. [[CrossRef](#)]
33. He, F.; Wang, J.; Deng, D.; Cheng, J. Sintering Behavior of Bi₂O₃–ZnO–B₂O₃ System Low-melting sealing Glass. *J. Chin. Ceram. Soc.* **2009**, *37*, 1791–1795. [[CrossRef](#)]



© 2020 by the authors. Licensee MDPI, Basel, Switzerland. This article is an open access article distributed under the terms and conditions of the Creative Commons Attribution (CC BY) license (<http://creativecommons.org/licenses/by/4.0/>).